Activated Protein C blocks the inhibitory effect on neurite outgrowth by extracellular histones that mediates its inhibition through a retrograde YB-1 signal

Short title: Activated Protein C blocks the inhibitory effect on neurite outgrowth by extracellular histones

Mustafa M. Siddiq[1,2], Sari S. Hannila[1,3], Yana Zorina[2], Elena Nikulina[1], Vera Rabinovich[2], Jianwei Hou[1], Rumana Huq[2], Erica L. Richman[1], Rosa E. Tolentino[2], Stella E. Tsirka[4], Ian Maze[5], Ravi Iyengar[2]* and Marie T. Filbin[1]*#

[1]Department of Biological Sciences, Hunter College, City University of New York NY, 10065

*Co-Senior Authors #Deceased January 15, 2014

[2]Department of Pharmacological Sciences and Systems Biology Center New York , Icahn School of Medicine at Mount Sinai , New York , NY, 10029

[3]Department of Human Anatomy and Cell Science, Rm 130, Basic Medical Sciences Building, 745 Bannatyne Ave, Winnipeg, Manitoba R3E 0J9

[4]Department of Pharmacology, University Medical Center at Stony Brook, NY 11794-8651

[5]Department of Neuroscience, Icahn School of Medicine at Mount Sinai, New York , NY, 10029.

Address correspondences to:

Ravi Iyengar

Dept of Pharmacological Sciences, Box 1215

1425 Madison Rm 12-70

New York NY 10029

Ravi.iyengar@mssm.edu

And Mustafa M. Siddiq

Mustafa.siddiq@mssm.edu

Supported by NIH post-doctoral fellowship award F32 NS054511-03 awarded to MMS, SNRP GRANT #NS041073, RCMI-NIH G12 and NIH 5 R01NS37060-14 awarded to MTF, NIH grants R01GM54508 and Systems Biology Center grant P50GM071558 awarded to RI.

One sentence summary: Proteins typically associated with chromatin structure play an unexpected role in limiting axonal regeneration after injury.

Abstract

Axonal regeneration in the mature CNS is limited by inhibitory factors within the extracellular environment. In this study, we show that histones H3 and H4 inhibit neurite outgrowth when applied to cortical neurons *in vitro*, and that this effect can be reversed by the addition of activated protein C (APC). Elevated levels of histones H3 and H4 were also detected in cerebrospinal fluid following CNS injury, and treatment with APC significantly increased axonal regeneration. Mechanistically, we have determined that histones activate a retrograde signaling cascade that results in phosphorylation of the transcription factor YB-1, and that neurite outgrowth is impaired when YB-1 is overexpressed in cortical neurons. These findings identify extracellular histones as a new class of growth-inhibiting molecules within the injured CNS.

Main Text

CNS myelin proteins and chondroitin sulfate proteoglycans (CSPGs) are well-characterized inhibitors of axonal growth (1-4), but genetic and pharmacological elimination of these factors elicits only a modest increase in axonal regeneration following spinal cord injury (5). This suggests that other inhibitory molecules are present in the CNS environment. Extracellular histones have been detected in neurodegenerative diseases such as Alzheimer's disease, scrapie, and Parkinson's disease (6-8), and histone H1 has been shown to induce microglial activation and neuronal apoptosis. It has also been reported that histones are released from apoptotic and necrotic cells following cerebral ischemia, lung injury, and myocardial infarction (7, 9). As ischemia and cell death are key pathophysiological events in spinal cord injury, we hypothesized that levels of extracellular histones would increase in response to trauma and that these proteins may play a role in regenerative failure.

To determine whether extracellular histones are elevated following spinal cord injury, we performed T8-9 level dorsal column lesions in 9-12 weeks old 129S1/SvImJ mice (The Jackson Laboratory) and collected cerebrospinal fluid (CSF) from the injury site 24 hours later. When compared to a sham group that received laminectomy alone, histone levels were significantly higher in CSF obtained from spinal cord-injured animals (Figs. 1E&F). To provide further evidence of histone release after CNS injury, we exposed the optic nerve in adult rats and placed gelfoam on the uninjured nerve. These pre-injury gelfoam samples were extracted 48 hours later. The nerve was then re-exposed and crushed and a new piece of gelfoam was placed at the injury site for 48 hours. Western blot analysis revealed that histone levels were visibly increased in the

optic nerves of individual animals following injury, and overall, this increase was statistically significant (Figs. 1G&H). We looked at histones released in gelfoam in the same animal (N=6) with (Post-ONC) and without (Pre-ONC) optic nerve crush (ONC) and have put them in Table 1.

To assess the effects of extracellular histones on axonal growth, we then performed a series of neurite outgrowth assays. P1 rat cortical neurons were plated on monolayers of primary rat astrocytes, and treated with a mixed population of histones isolated from calf thymus (1-20 μg/ml). Neurite outgrowth was significantly reduced in a dose-dependent manner in response to histone treatment (Fig. 1A and S1A). This effect was not due to toxicity or the presence of other inhibitory factors, as the astrocyte monolayers were unaffected by the histones (Figs. 1B), and histones did not induce expression of the CSPGs neurocan and brevican in astrocytes (Fig. S1B). Using permissive substrates of Chinese hamster ovary (CHO) cells, we observed that histones inhibited neurite outgrowth in a dose-dependent manner for both cortical (Figs. 1C&D and S2) and dorsal root ganglion neurons (Fig. S3), and that treatment with dibutyryl cyclic AMP could reverse this inhibition (Figs. 1D&S2). In addition, when neurons were treated with fatty acid binding protein, which has a similar size and isoelectric point (but no homology) to histones, neurite outgrowth was unaffected (Figs. 1D&S2B). This indicates that the inhibition that was observed was histone-mediated, and not due to non-specific steric hindrance. Finally, to elucidate the contributions of specific core histones to inhibition, cortical neurons were plated in microfluidic chambers, and recombinant histones H3 and H4 were applied to the neurite compartment. Both histone H3 and H4 inhibited neurite outgrowth, with histone H3 having a more potent effect (Fig. 1I).

Morphologically, neurites treated with either histone H3 or H4 displayed the prominent end bulbs typical of dystrophic axons (Figs. 1I', Fig. S4).

Previous studies have reported that the deleterious effects of extracellular histones can be attenuated by activated protein C (APC), a coagulation factor that has been shown to specifically cleave histones H3 and H4 (6), and enhance neuroprotection in cerebral ischemia (10). Using cortical neurons plated in microfluidic chambers, we observed that administration of APC blocked histone-mediated inhibition of neurite outgrowth (Fig. 2A, 2B). To determine if APC could promote axonal regeneration *in vivo*, APC-containing gelfoam was applied to the injury site following ONC in rats. Retinal ganglion cell axons were anterogradely labeled with cholera toxin B-subunit (CTB) at 14 days after injury, and optic nerves were chemically cleared using the 3-DISCO technique (11). Crush sites were identified using a novel technique, the second harmonic generation, which allows visualization of collagen fibrils (Figs. 2G,G',H&H') (Figs. S5A) (12&13), and axonal regeneration was quantified by fluorescent intensity from the crush site at 100micron increments (Fig. 2E) volumetric analysis of CTB-labeled axons (Figs. 2F & S5B&C). Control animals treated with saline-containing gelfoam had limited and short CTB-labeled axons crossing the lesion site (Fig. 2C, 2E). In APC-treated animals, however, we observed a significant increase in axonal regeneration beyond the site of injury (Figs. 2D, 2E).

To elucidate the molecular mechanism underlying histone-mediated inhibition of neurite outgrowth, we treated cortical neurons with histones for 24 hours and then plated them onto permissive CHO cell monolayers in the absence of histones (14). Neurite outgrowth was severely impaired in these neurons (Fig. S6), which suggested that their

intrinsic capacity for neuritogenesis had been altered at the molecular level by the histones. To determine if this effect involved the activation of transcription factors, we incubated cortical neurons with extracellular histones for 30 or 120 minutes and analyzed the lysates using a Panomics Transcription Factor protein array (15). This assay revealed significant increases in eukaryotic Y-box-binding protein-1 (YB-1) in histone-treated neurons (Fig. S7), and we subsequently demonstrated that YB-1 expression has a direct impact on neurite outgrowth, as overexpression of YB-1 in cortical neurons resulted in shorter neurites compared to controls (Fig. 3B). We also showed that histones H3 and H4, as well as mixed histones, can induce phosphorylation of YB-1 (Fig. 3A). In our previous experiments we demonstrated that application of histones to distal neurites is sufficient to inhibit neurite outgrowth (Figs. 1I&2A), and this suggests that histones may induce phosphorylation of YB-1 through retrograde signaling. To test this hypothesis, the neurite compartments of microfluidic chambers were treated with histones coupled to 6 µm silicone beads, which prevents their diffusion into the somal compartment, while preserving their ability to interact with the neurites. When the histone-conjugated beads were applied to the neurites, we observed increased pYB-1 levels in the neuronal cell bodies, confirming a retrograde signal (Fig. 4C). Interestingly, the neurites treated with the histone-conjugated beads displayed prominent varicosities (Fig. 3D2&4, while neurites treated with unconjugated beads were unaffected (Fig. 3D1&3.). This not only demonstrates that the beads had no toxic effects, but also provides further evidence that histones negatively affect axonal function and integrity, as these varicosities are indicative of disruptions in axonal transport and impending degeneration. Finally, to determine if retrograde induction of YB-1 phosphorylation occurs *in vivo*, we performed

optic nerve crushes and collected the ipsilateral and contralateral retinas 48 hours later. We observed baseline phosphorylation of YB-1 in the contralateral retina, and this was visibly increased in response to optic nerve crush (Fig. 3E). These results demonstrate that CNS injury can induce YB-1 phosphorylation in neurons and given our data showing that histone levels are elevated following optic nerve crush (Fig. 1H), it is highly probable that this occurs through histone-mediated retrograde signaling.

Histones lie at the very core of chromatin structure and function, but here we show that they have a very different role outside the nucleus. Histones are released into the extracellular environment following CNS injury, and they act as potent inhibitors of axonal regeneration both *in vitro* and *in vivo*. Extracellular histones produce a degree of inhibition that is comparable to that elicited by myelin-associated inhibitors and CSPGs (16,17), and we therefore propose that histones should be considered a third major class of inhibitory molecules within the CNS. Eliminating inhibitory factors from the CNS environment has been widely used as a strategy to enhance axonal regeneration, but the results have often been underwhelming. Triple mutant mice lacking expression of myelin-associated glycoprotein (MAG), Nogo, and oligodendrocyte myelin glycoprotein did not exhibit spontaneous regeneration of corticospinal and raphespinal axons after spinal cord injury (5). Similarly, elimination of CSPGs through treatment with chondroitinase ABC (chABC) resulted in only modest regeneration of dorsal column and corticospinal axons (maximum of 4 mm) following dorsal column lesions (18). The presence and persistence of extracellular histones at the site of injury could therefore account for the limited axonal regeneration that was observed in these studies.

Having established that histones inhibit axonal regeneration, we must now consider their mechanism of action, and our observation that APC can block the effects of histones provides some initial insight. Since APC functions by cleaving histones, this indicates that histone proteins are directly responsible for mediating inhibition. This is further supported by our observation that APC cannot overcome inhibition by MAG in a neurite outgrowth assay (Fig. S8), which demonstrates that APC does not enhance growth through non-specific degradation of other proteins or effects on the neurons themselves. Our results also show that histones induce phosphorylation of YB-1 through retrograde signaling, which suggests that this effect is receptor-mediated. Histones have been shown to activate intracellular signaling by binding to cell-surface receptors such as Toll-like receptors 2 and 4 (19), and intriguingly, there is a demonstrated connection between TLR4 and YB-1, as TLR4 expression was reduced in YB-1 heterozygous mice (20). This raises the possibility that histones may induce the expression and phosphorylation of YB-1 within neurons by binding to TLR4.

Studies of myelin-associated inhibitors and CSPGs have shown that these molecules inhibit axonal regeneration through activation of the small GTPase RhoA (21). We observed that extracellular histones activated RhoA in similar manner (Fig. 3F) and they also reduced levels of p35 (Figs. 3G), a protein that can overcome MAG-mediated inhibition by activating cyclin-dependent kinase 5 (22). This provides evidence that the signaling pathways activated by CNS myelin, CSPGs, and histones converge at key points to mediate inhibition, and importantly, it also shows that histones can affect cytoskeletal dynamics. It has been reported that YB-1 can promote microtubule

assembly (23), and so it is possible that histones may activate RhoA through phosphorylation of YB-1.

The addition of histones to the list of inhibitory molecules in the CNS reinforces the prevailing view that combinatorial therapies will be necessary to promote axonal regeneration and functional recovery following spinal cord injury. Elevation of intracellular cyclic AMP can overcome inhibition by myelin-associated inhibitors and CSPGs, and we have found that it can reverse inhibition by histones as well (24&25), which suggests that rolipram or other phosphodiesterase inhibitors could be an effective way to target all three classes of inhibitors. Histones could also be neutralized using APC, which would digest the histones within the lesion site and create a more permissive environment for regeneration. It should be noted that this treatment would not affect histones in intact cells, which means that APC would likely have minimal adverse effects *in vivo*. This approach could be particularly effective when used in combination with chABC and other interventions that modify the extracellular environment, such as cell transplantation. The findings presented in this study add another layer of complexity to the challenge of promoting axonal regeneration in the CNS, but they also reveal new opportunities for progress in both fundamental and translational neuroscience that could greatly advance the treatment of spinal cord injury.

Methods

Rat primary cortical or hippocampal neuron cultures – Rat primary cortical cultures were dissected from postnatal day 1 Sprague Dawley rat brains. Cortices or hippocampi were incubated for 30mins (once for hippocampi and twice for cortices) with 0.5 mg/ml papain (Sigma) in plain Neurobasal (NB) media (Invitrogen) with DNase. Papain activity was inhibited by brief incubation in soybean trypsin inhibitor (Sigma). Cell suspensions were layered on an Optiprep density gradient (Sigma) and centrifuged at 1900 x *g* for 15mins at room temperature. The purified neurons were then collected at 1000 x g for 5 mins and counted.

Primary cortical neurons were diluted to 35,000 cells/ml in NB supplemented with B27, L-glutamine and antibiotics and grown for 24hours. To quantify the outgrowth we immunostained using a monoclonal anti-βIII tubulin antibody (Tuj1;Covance) and Alexa Fluor 568-conjugated anti-mouse IgG (Invitrogen). For quantification, images were taken, and the length of the longest neurite for each neuron was measured using MetaMorph software (Molecular Devices). For western blots primary neurons were lysed in radioimmunoprecipitation assay (RIPA) buffer (50mM Tris-HCl, pH 7.5; 100mM NaCl; 1 % Nonidet P-40; 0.5 % deoxycholic acid; 0.1 % SDS; 1mM EDTA) supplemented with protease and phosphatase inhibitors. After determination of protein concentration, the cell lysates were subjected to immunoblot analysis using standard procedures and visualized by enhanced chemiluminescence (ECL). Polyclonal rabbit antibodies directed against p35, phospho-YB-1 or total YB-1 were from Cell Signaling Technology Inc.

Rat primary dorsal root ganglion neurons – Rat dorsal root ganglion (DRG) neurons from extracted from P5-P7 day old pups. The neurons were first treated with with 0.015% collagenase in Neurobasal-A media for 45 min at 37°C. This was followed by a second incubation in

collagenase for 30 min at 37°C, with the addition of 0.1% trypsin and 50 µg/ml DNase I. Trypsin was inactivated with DMEM containing 10% dialyzed fetal bovine serum. The ganglia were triturated in Sato's media and counted.

Rat primary astrocytes- We prepared mixed cortical cultures from P3-P5 pups. The cortices were removed and the meninges carefully peeled away. They were treated with 0.1% trypsin and 50 µg/ml DNase I for ten minutes at 37°C. Trypsin was inactivated with DMEM containing 10% dialyzed fetal bovine serum (FBS). We triturated the tissue and strained the cell suspension which was seeded into a pre-coated PLL T75 tissue flask in the growth media of DMEM with 10%FBS. Media was replaced within 24hrs and then every 3 days until we had a confluent layer of cells (10-14 days). To enrich for astrocytes, the media was replaced with plain NB (no supplements but containing Hepes) and we shaked the culture at 200RPM at 37°C. The media and floating cells were aspirated off and we added fresh DMEM with 10%FBS and returned to the incubator overnight. The next day we would trypsinize the remaining cells for for ten minutes at 37°C, or longer depending on how the cells are lifting off the flask. Trypsin was inactivated with DMEM containing 10% dialyzed fetal bovine serum, and the astrocytes were counted.

Neurite outgrowth assay. Mono layers of permissive control or MAG-expressing Chinese hamster ovary (CHO) cells or primary astrocytes were plated on eight well chamber slides as previously described (26). Purified P1 hippocampal, P1 cortical, P5–P6 CGN, or P5–P6 DRG rat neurons were diluted to 35,000 cells/ml in Sato's media and treated with either 1 mM dbcAMP (Calbiochem), mixed population or recombinant Histones (1-20µg/ml) or with APC (1-20µg/ml). Neurons were incubated for 14–18 h at 37°C and immunostained using a monoclonal anti-βIII tubulin antibody (Tuj1;Covance) and Alexa Fluor 568-conjugated anti-mouse IgG (Invitrogen).

For quantification, images were taken, and the length of the longest neurite for each neuron was measured using MetaMorph software (Molecular Devices).

Microfluidic neurite outgrowth assay- Square microfluidic chambers (150 or 450 microgroove) were purchased from Xona microfluidics. The chambers were sterilized under UV for 15mins and soaked in 70% ethanol for 2mins and allowed to air dry under a sterile TC hood. We used MatTek dishes (P50G-1.5, MatTek corp.) that we pre-coat with PLL overnight, rinse 3 times with sterile water and air dry overnight in a sterile hood. Using sterile foceps we carefully place the microfluidic chamber on the glass area of the MatTek dish, and gently apply pressure to ensure the chambers are sitting on the glass. 3 whole brain P1-2 cortices after papain enzymatic digestion and Optiprep gradient are resuspended in 200µls of NB with full supplements. We then seed 15µls of the neuronal suspension on one side of the microgroove and place in a 37°C incubator for 20mins to allow the neurons to adhere. All wells are filled with 150µls of supplemented NB. Once we observe neurites growing across the microgroove (2-3days), we then do our treatments on the neurite compartment and wait 48hrs before we add 4% Paraformaldehyde with 4%Sucrose. We use the Neon transfection (Invitrogen) method to overexpress the plasmid YB-1.

Rho Activation Assay. Rat cortical neurons plated in 10cm^2 dishes (approximately 10 million neurons per dish) were used with a commercially available Rho Activiation Assay Kit (Millipore). The neurons were placed in plain NB media for 4hrs prior to assay. In brief, following the manufacturers protocol, we lysed the cortical neurons on ice with MLB buffer supplemented with anti-protease and anti-phosphatase cocktails (Calbiochem) and spun the lysates at 14,000 x g for 5 mins. The supernatant was collected and added to 35µls of agarose beads coupled to Rhotekin Rho Binding Domain and rocked in the cold room for 45mins, a small

sample of each supernatant was not added to the beads and was used as total Rho loading controls. Beads were washed three times with MLB buffer and 20µls 2xLaemmeli buffer was added and samples were prepared for western blotting. Proteins were separated on pre-cast 4-20% gradient gels (Thermo Fisher Scientific) and transferred to nitrocellulose at 75V for 1 hr. Membranes were successfully probed with rabbit anti-RhoA (1:1000; Cell Signaling Technology) and HRP conjugated anti-rabbit IgG (1:2000; Cell Signaling Technology). Membranes were reacted with Pierec ECL Western Blotting Substrate or SugperSignal West Femto Maximam Sensitivity Substrate (Thermo Fisher Scientific). Densitometirc measurements were made using NIH Image J software.

Rat optic nerve regeneration in vivo:

Optic nerve crush experiments. Adult male or female Sprague-Dawley or rats (250–280 g, approximately 8-10 weeks old) were anesthetized with isoflurane and placed in a stereotaxic frame. The right optic nerve was exposed and crushed with fine forceps for 10s. We placed gelfoam either soaked in PBS or with APC [4.1mg/ml] (Haematologic Technologies, Inc) were placed over the injury site. 3 days prior to sacrificing we label the regenerating axons with 5µls of 1mg/ml Cholera Toxin B (CTB) coupled to Alexa-488 which we intravitreally inject. Animals were anesthetized with ketamine (100mg/kg) and xylazine (20mg/kg) injected intraperitoneally and transcardial perfusion with 4% PFA after a 14 days postsurgical survival period. When animals are deeply anesthetized we will transcardially perfuse with cold 4%Paraformaldehyde (PFA) in PBS, pH 7.4. The optic nerves and chiasm attached will be dissected out and post-fixed in 4%PFA overnight at 4^{o}C, rinsed for one hour in PBS and then we prepare them for chemical clearing. Since the advent of the 3DISCO clearing techniques, we are no longer dependent on

sectioning the tissue, this method also eliminates bias associated with artifacts produced by sectioning. The whole nerve is placed in a graded series dehydration technique in Tetrahydrofuran (THF;Sigma) diluted in water: 50%,70%,80%,100% and 100% again. Each THF dilution is for 20mins at room temperature on an orbital shaker (25). Followed by Dicholoromethane (Sigma) for 5mins at room temperature on an orbital shaker and followed by the clearing agent, Dibenzyl ether (DBE; Sigma) overnight at room temperature on an orbital shaker. Microscope slides are mounted with Fastwell chambers (Electron Microscopy Sciences) and the cleared sample is place on the slide and covered with DBE, a No. 1.5 micro cover glass is used the cover the sample. We image the whole sample on an Olympus Multiphoton microscope with a 25X water immersion lens. All procedures were approved by the IACUC of the Icahn School of Medicine at Mount Sinai in accordance with NIH guidelines. All procedures were approved by the IACUC of the Icahn School of Medicine at Mount Sinai in accordance with NIH guidelines. Multiphoton microscopy was performed in the Microscopy CORE at the Icahn School of Medicine at Mount Sinai and was supported with funding from NIH Shared Instrumentation Grant 1S10RR026639-01.

Multiphoton Image Analysis:

Images were deconvolved using AutoQuant X Software (Media Cybernetics). Deconvolved images were then analyzed using Amira Software version 6.0.1 (Thermo Scientific). Z-stacks were uploaded to create a 3D volume rendering of the crush site and labelled neurites. For samples containing more than one Z-stack, image stacks were aligned and merged using Amira's merge module. The images were then rotated to position the crush site proximal to the retina on the left with regenerated neurites growing away from the crush site towards the right. The transformed data was resampled and axes swapped such that the XY plane became the cross

section along the length of the nerve. Images were cropped if needed to exclude any partial cross sections of the ends of the nerve caused by image rotation. Labelled regenerated neurites were segmented by thresholding pixels using Amira's Segmentation Editor. The volume ratio of segmented neurites over total nerve volume was measured for each sample. Study results were then normalized and plotted in a bar graph.

The ratio of segmented area over total nerve area for each cross section was normalized and plotted as area ratio per slice. Area ratio plots were created starting from the behind the crush site proximal to the retina and following along the length of the nerve for the segmented regenerated neurites.

Cell fractionation and Panomics transcription factor activation arrays- Nuclear and cytosolic extracts were isolated from cortical neurons following instructions from a commercial kit (Pierce). The supernatant containing the nuclear extract was used in a Panomics Combo Protein-DNA Array (Affymetrix, MA1215) to study transcription factor activation following the manufacturer's protocol. The array was visualized by enhanced chemiluminescence and determined where we had a positive signal.

Statistical analyses. All analyses were performed using GraphPad Prism software, and data are represented as mean ± SEM. Statistical significance was assessed using paired one-tailed Student's *t* tests to compare two groups, and one-way ANOVAs with Bonferroni's *post hoc* tests to compare between three or more groups.

References

1. Filbin, MT (2004). Myelin-associated inhibitors of axonal regeneration in the adult mammalian CNS. Nat. Rev. Neurosci. 4, 703-13.
2. Buchli AD and Schwab ME (2005). Inhibition of Nogo: a key strategy to increase regeneration, plasticity and functional recovery of the lesioned central nervous system. Ann. Med. 37, 556-67.
3. Galtrey, CM and Fawcett, JW (2007). The role of chondroitin sulfate proteoglycans in regeneration and plasticity in the central nervous system. Brain Res. Rev. 54, 1-18.
4. He Z and Jin Y (2016). Intrinsic Control of Axon Regeneration. Neuron 90, 437-51.
5. Cafferty WB, Duffy P, Huebner E and Strittmatter SM (2010). MAG and OMgp synergize with Nogo-A to restrict axonal growth and neurological recovery after spinal cord trauma. J Neurosci. 30, 6825-37.
6. Xu J, Zhang X, Pelayo R, Monestier M, Ammollo CT, Semeraro F, Taylor FB, Esmon NL, Lupu F and Esmon CT (2009). Nat. Med. 15, 1318-21.
7. Non-nuclear histone H1 is upregulated in neurons and astrocytes in prion and Alzheimer's diseases but not in acute neurodegeneration (1999). Neuropathology and Applied Neurobiology 25, 425-432.
8. Gilthorpe JD, Oozeer F, Nash J, Calvo M, Bennett DLH, Lumsden A and Pini A (2013). Extracellular histone H1 is neurotoxic and drives a pro-inflammatory response in microglia. F1000 Research 2:148. Doi: 10.12688/f1000research.2-148.v1.
9. DeMeyer SF, Suidan GL, Fuchs TA, Monestier M and Wagner DD (2012). Extracellular chromatin is an important mediator of ischemic stroke in mice. Arterioscler. Thromb. Vasc. Biol. 32, 1884-1891.
10. Griffin JH, Fernández JA, Lyden PD and Zlokovic BV (2016). Activated protein C promotes neuroprotection: mechanisms and translations to the clinic. Thrombosis Research 141S2, S62-S64.
11. Ertürk A, Mauch CP, Hellal F, Förstner F, Keck T, Becker K, Jährling N, Steffens H, Richter M, Hübener M, et al. (2012). Three-dimensional imaging of the unsectioned adult spinal cord to assess axon regeneration and glial responses after injury. Nat. Med. 18, 166-171.
12. Freund I, Deutsch M and Sprecher A (1986). Optical Second-harmonic Microscopy, Crossed-beam Summation, and Small-angle Scattering in Rat-tail Tendon. Biophys. J. 50, 693-712.
13. Vijayaraghavan S, Huq R and Hausman MR (2014). Methods of peripheral nerve tissue preparation for second harmonic generation imaging of collagen fibers. Methods 66, 246-255.
14. Cai D, Shen Y, De Bellard M, Tang S and Filbin MT (1999). Prior exposure to neurotrophins blocks inhibition of axonal regeneration by MAG and myelin via a cAMP-dependent mechanism. Neuron 22, 89-101.
15. Bromberg KD, Ma'ayan A, Neves SR and Iyengar R (2008). Design logic of a cannabinoid receptor signaling network that triggers neurite outgrowth. Science 320, 903-9.
16. Siddiq MM, Hannila SS, Carmel JB, Bryson JB, Hou J, Nikulina E, Willis MR, Mellado W, Richman EL, Hilaire M, Hart RP and Filbin MT (2015). Metallothionein-I/II Promotes Axonal Regeneration in the Central Nervous System. J. Biol. Chem. 290, 16343-16356.

17. Shen Y, Tenney AP, Busch SA, Horn KP, Cuascut FX, Liu K, He Z, Silver J and Flanagan JG (2009). PTPσ Is a Receptor for Chondroitin Sulfate Proteoglycan, an Inhibitor of Neural Regeneration. Science 326, 592-96.
18. Bradbury EJ, Moon LD, Popat RJ, King VR, Bennett GS, Patel PN, Fawcett JW and McMahon SB (2002). Chondroitinase ABC promotes functional recovery after spinal cord injury. Nature 416, 636-40.
19. Marsman G, Zeerleder S and Luken BM. Extracellular histones, cell-free DNA, or nucleosomes: differences in immunostimulation (2016). Cell Death Dis. 7, e2518.
20. Hanssen L, Alidousty C, Djudjaj S, Frye BC, Rauen T, Boor P, Mertens PR, van Roeyen CR et al. (2013). YB-1 Is an Early and Central Mediator of Bacterial and Sterile Inflammation In Vivo. J. Immunol. 191, 2604-13.
21. Lehmann M, Fournier A, Selles-Navarro I, Dergham P, Sebok A, Leclerc N, Tigyi G and McKerracher L (1999). Inactivation of Rho signaling pathway promotes CNS axon regeneration. J. Neurosci. 19, 7537-47.
22. He H, Deng K, Siddiq MM, Pyie A, Mellado W, Hannila SS and Filbin MT (2016). Cyclic AMP and Polyamines Overcome Inhibition by Myelin-Associated Glycoprotein through eIF5A-Mediated Increases in p35 Expression and Activation of Cdk5. J. Neurosci. 36, 3079-3091.
23. Chernov KG, Mechulam A, Popova NV, Pastre D, Nadezhdina ES, Skabkina OV, Shanina NA, Vasiliev VD et al. (2008). YB-1 promotes microtubule assembly in vitro through interaction with tubulin and microtubules. BMC Biochemistry 9, 23.
24. Cai D, Shen Y, De Bellard M, Tang S and Filbin MT (1999). Prior exposure to neurotrophins blocks inhibition of axonal regeneration by MAG and myelin via a cAMP-dependent mechanism. Neuron 22, 89-101.
25. Lu P, Yang H, Jones LL, Filbin MT and Tuszynski MH (2004). Combinatorial therapy with neurotrophins and cAMP promotes axonal regeneration beyond sites of spinal cord injury. J. Neurosci. 24, 6402-9.
26. Mukhopadhyay G, Doherty P, Walsh FS, Crocker PR, Filbin MT (1994). A novel role for myelin-associated glycoprotein as an inhibitor of axonal regeneration. Neuron 13,757-67.

Figure 1

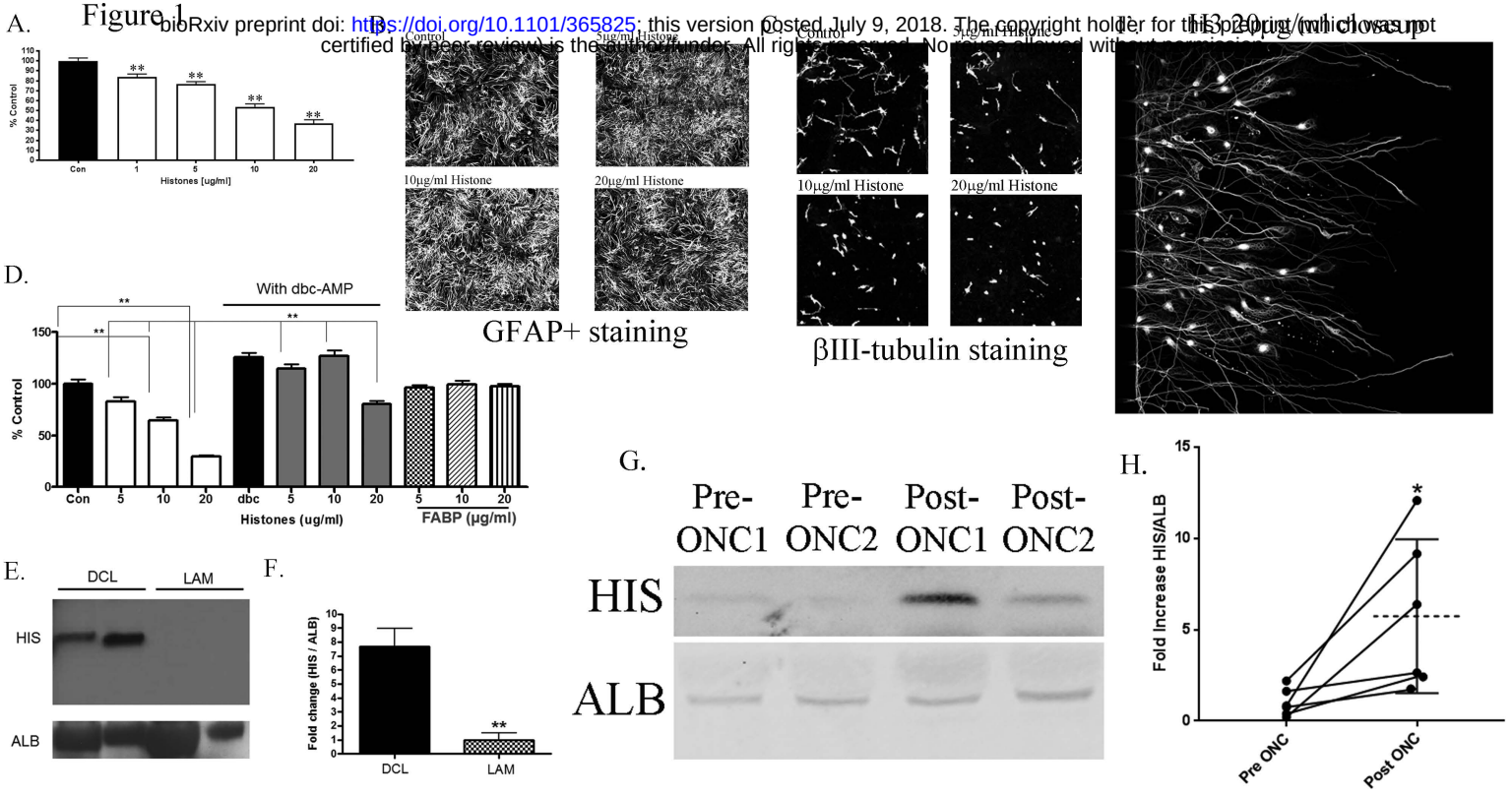

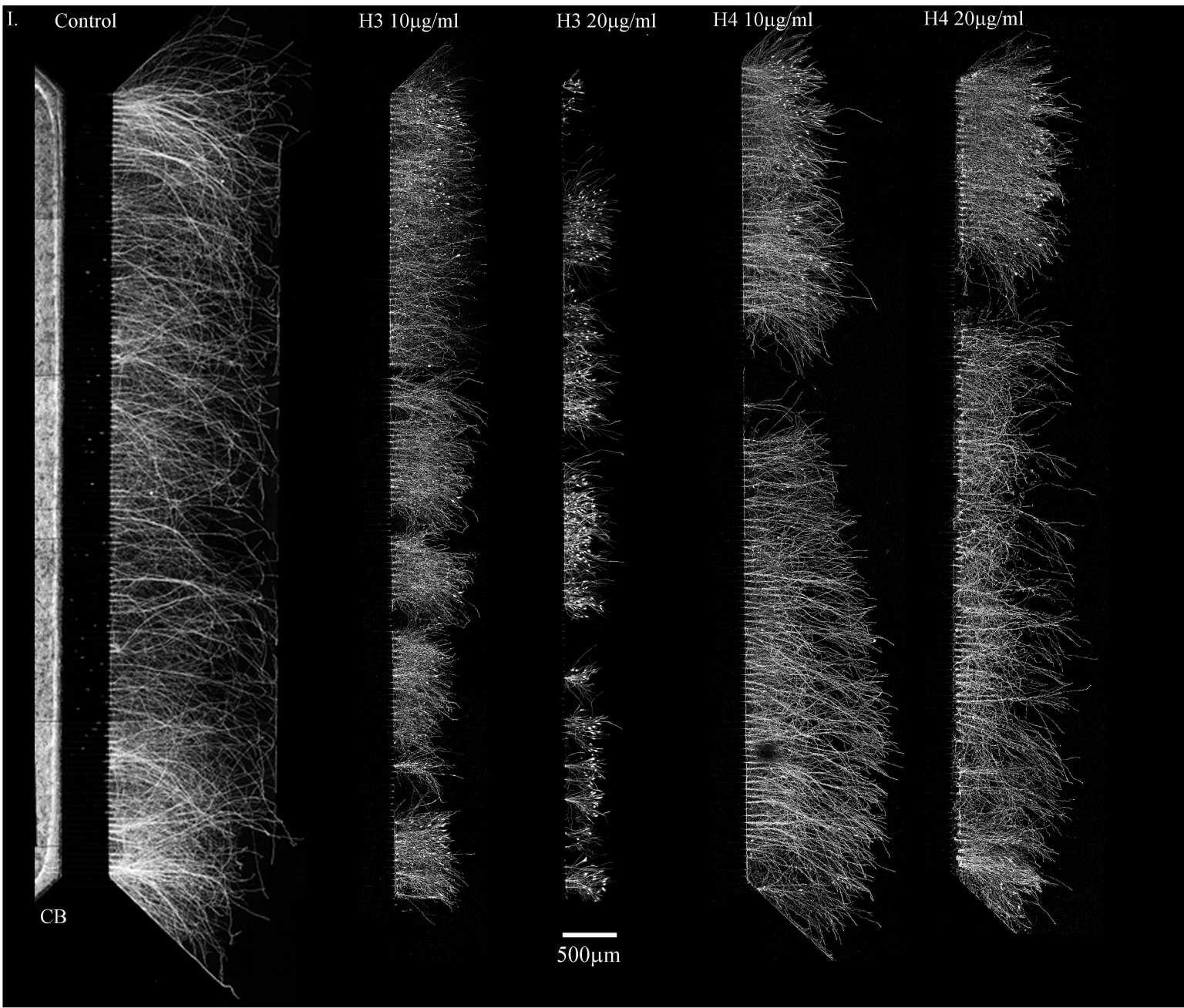

Figure 1 – Extracellular Histones are inhibitory to neurite outgrowth. A. Primary rat cortical neurons on an astrocytic monolayer put out long neurites (black bar) but in the presence of increasing concentrations of a mixed population histone preparation (white bars), they put out dose-dependent shorter neurites as determined by β-III tubulin staining and quantified longest length by Metamorph. This bar graph is the average of three independent experiments. B. Representative images of GFAP+ astrocytic monolayers in the absence or presence of 5-20μg/ml as indicated. C. Images of β-III tubulin+ cortical neurons on a monolayer of permissive CHO cells with or without histones as indicated. D. Cortical neurons on a permissive CHO monolayer put out long neurites (black bars, Con) but in the presence of histones they put out significantly shorter neurites (white bars). 1mM dbc-AMP alone (black bar labeled dbc) can overcome the inhibitory effect of the histones (grey bars, indicated combination of dbc-AMP and Histones in concentration noted). Using a control protein Fatty Acid Binding Protein (FABP) does not affect neurite outgrowth (black and white patterned bar graphs). E. Elevated levels of Histone H3 (HIS) in the CSF fluid collected from mice with DCL are detected by western blot, compared to laminectomy (LAM) alone. E. Histone H3 levels are normalized to Albumin (ALB) and in the bar graph is the average of 5 animals (n=5 for both DCL and LAM group) with DCL where we see a significant elevation of free Histone H3 in the CSF fluid. G. Adult rats first had their optic nerves exposed and we applied gelfoam over the uninjured nerve for 48hrs (Pre-ONC1&2), subsequently removing the gelfoam into PBS with protease inhibitor cocktail, we crushed the optic nerve and applied a fresh piece of gelfoam over the injury site. We removed the gelfoam 48hrs later (Post-ONC 1&2). We found within the same animal a significant increase in HIS levels after crushing the optic nerve (Post-ONC) than prior to injury (Pre-ONC), data was graphed in H. (n=6, see Table 1 for full comparison of Pre- and Post-ONC levels of HIS). I. Using PLL-coated microfluidic chambers, cortical neurons cell bodies (CB) grow long neurites across the 450μM microgroove as detected by β-III tubulin. Treating the neurite growing compartment with either recombinant H3 or H4 Histones resulted in significantly shorter neurites, with H3 having a more potent effect. I'. Looking at an enhanced region of the H3 20μg/ml treated side, the shorter neurites appeared to have dystrophic endbulbs. All statistics were performed by ANOVA, *$p<0.05$ and **$p<0.01$, except Figure F. was unpaired t-test and H. was paired t-test.

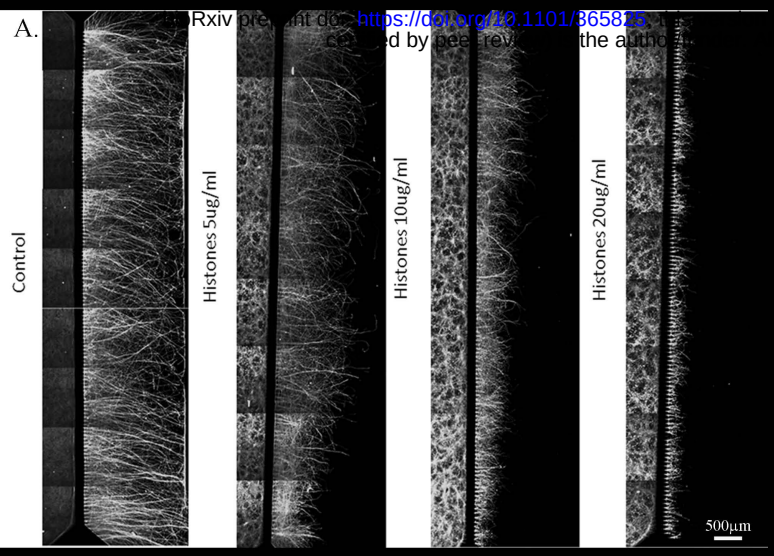

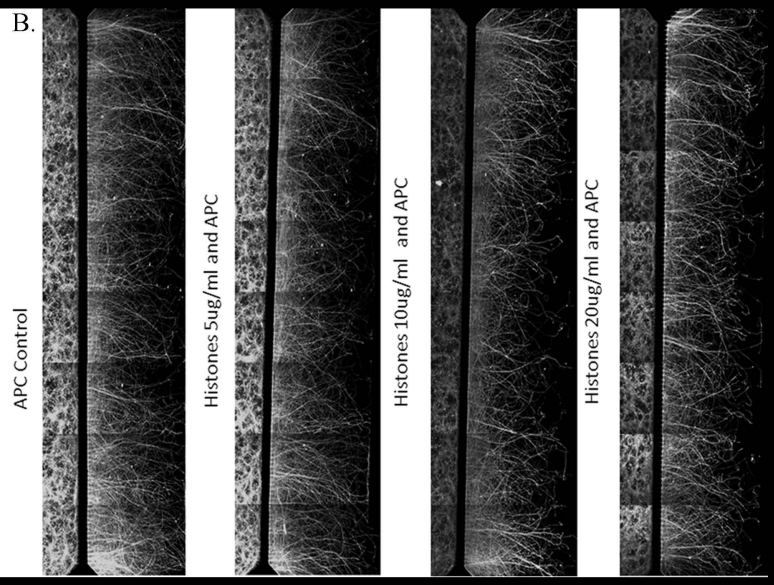

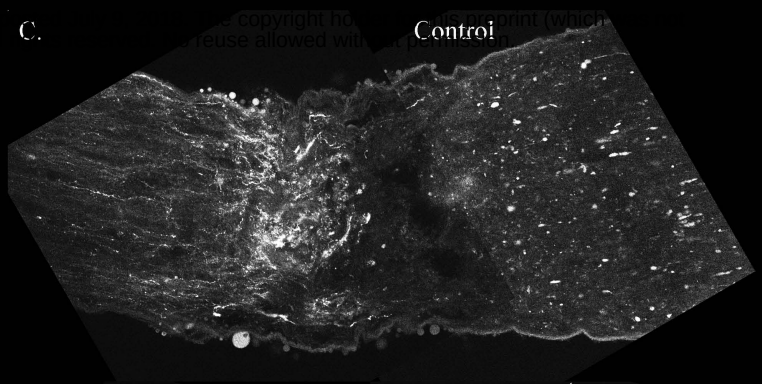

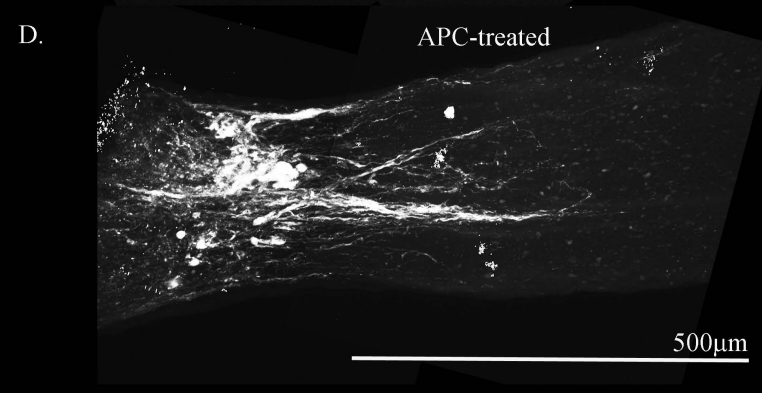

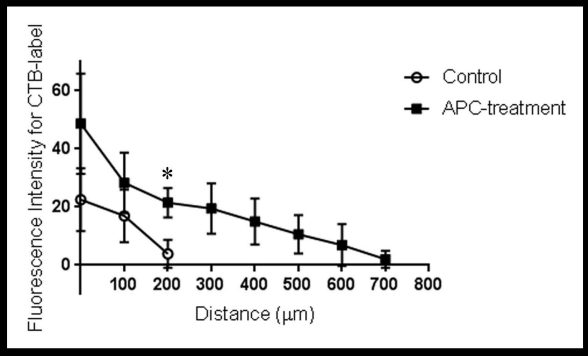

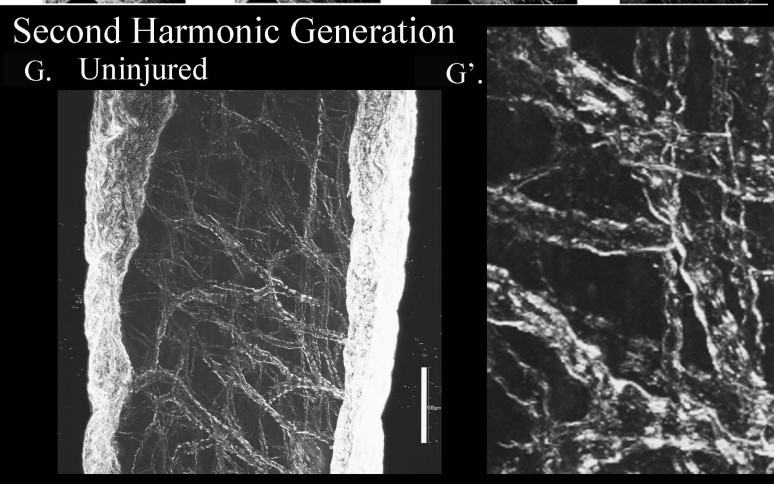

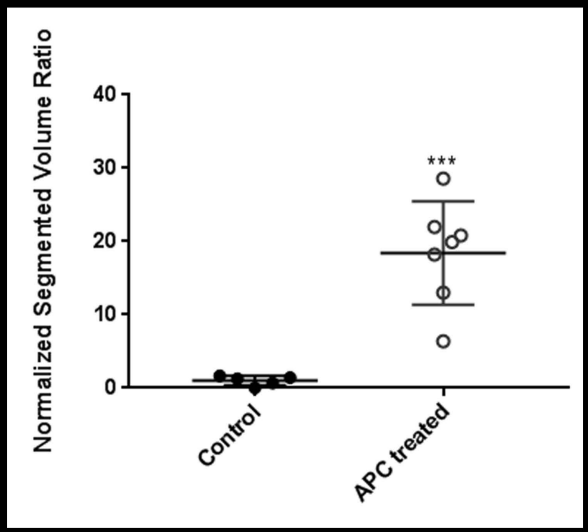

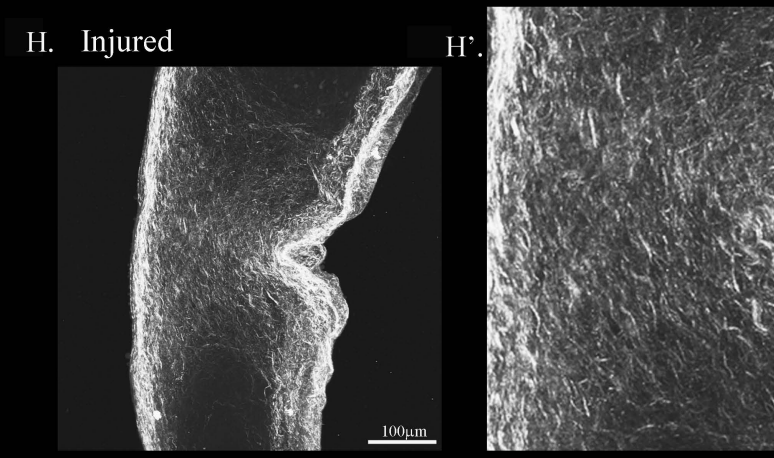

Figure 2

Figure 2 – APC blocks the inhibitory effect of Histones and promotes axonal regeneration after ONC. A. Cortical neurons plated on PLL coated microfluidic chambers grow robustly across the 150µm microgroove, determined by β-III tubulin staining. Treating the neurite growing side (right side from the microgroove) only with increasing concentrations of mixed population of histones results in significantly shorter neurites. **B.** APC alone has no effect on neurite outgrowth, combining APC with histones and applying to the neurite side reverses the inhibitory effect of histones, restoring long neurite outgrowth. **C.** Using the rat ONC model for axonal regeneration in the CNS, crushed axons without treatment (Control) have CTB labeled axons abruptly halt at the lesion site in this chemically cleared whole nerve. **D.** Representative optic nerve treated with APC soaked in gelfoam immediately after crushing the axons, the gelfoam is placed over the injury site. In this chemically cleared nerve CTB labeled axons are observed growing through the lesion site. Panel C & D are approximately 540 optical slices at 0.45µm increments that is merged together into a two-dimensional represented maximum projection intensity image. Scale bar of 500µm is for Figures C &D. **E.** Using Image J we quantitated the axonal regeneration for Control (n=5, white circle) and APC-treated (n=7, black square) every 100microns from the edge of the crush site. There is a significant difference in the extent of regeneration at 200microns, and no regenerating fibers were detected past that point in Control animals. **F.** Using Amira 3D maximum intensity projection of the nerve showing crush site and regenerating neurites labelled with CTB, we determined the Normalized Segmented Volume ratio. Line plot shows ratio of segmented neurite area over total nerve area per cross section along the nerve and we see a significant difference (***, $p<0.001$) with APC-treatment. Each cross section slice is .497 micrometers. **G.** Using Second Harmonic Generation imaging on Multi-photon microscope, collagen fibers auto-fluoresce. In uninjured whole chemically cleared nerves, we can see the collagen bundles, which the fibers are shown in enhanced detail in Figure **G'**. **H.** Injured optic nerves display crushed collagen fibers at the injury site, helping to elucidate the injury site and it is shown in an enhanced region in Fig. **H'**. Scale bar is 100µm in Figures G. and H.

Figure 3

A.

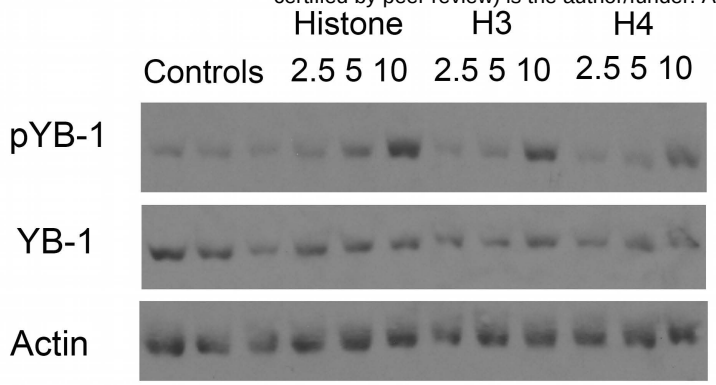

B.

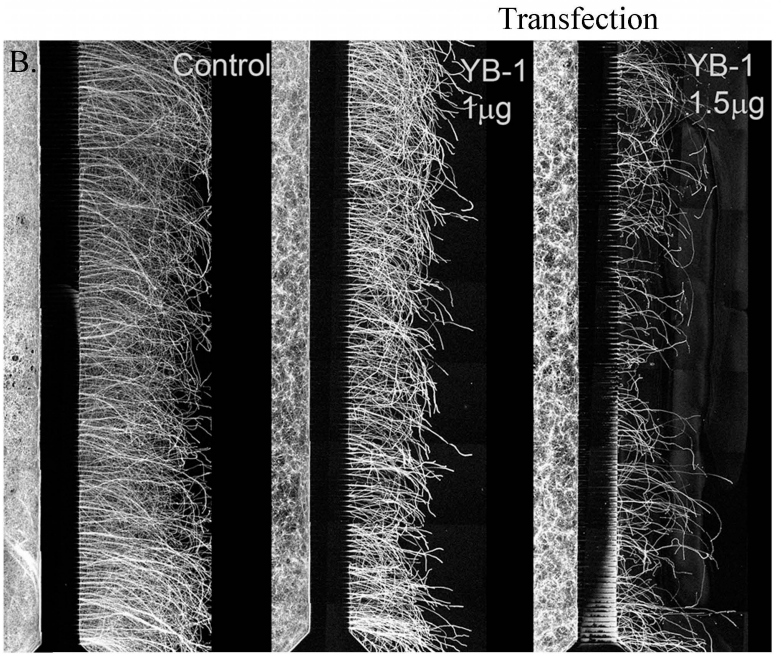

C.

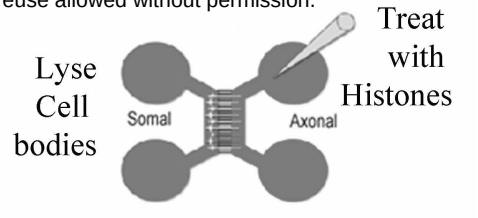

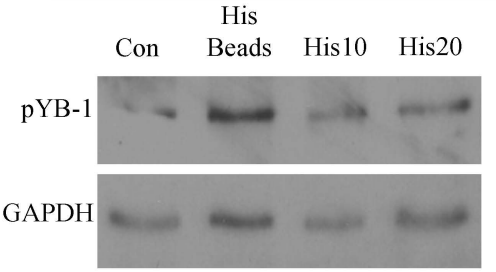

D1.

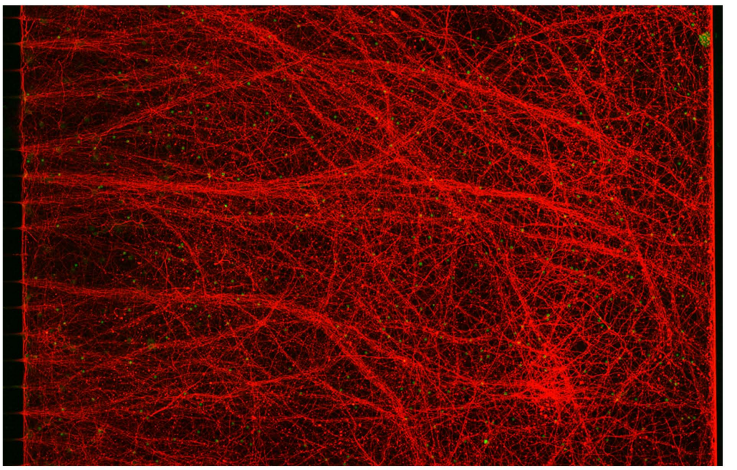

D2.

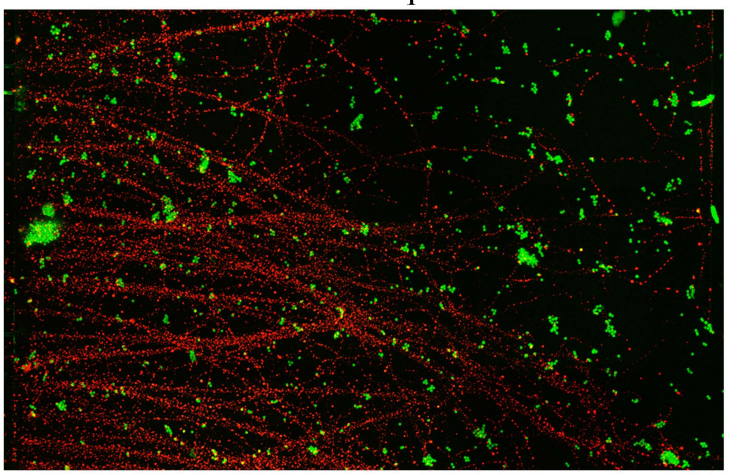

D3.

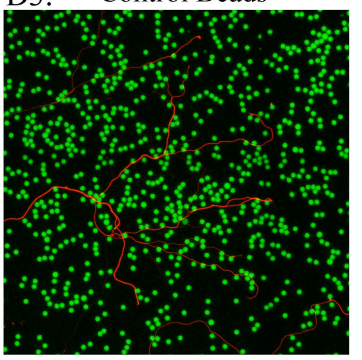

D4.

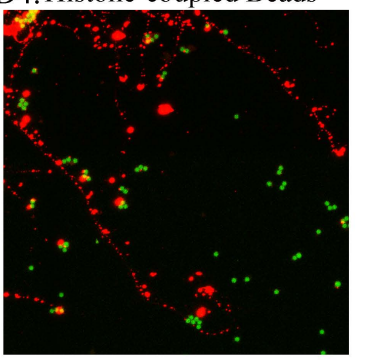

E.

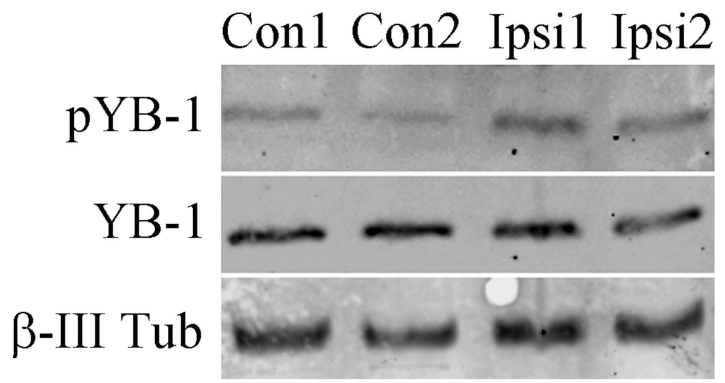

F.

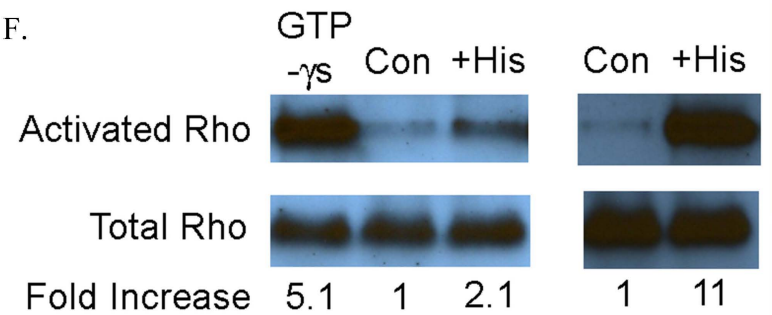

G.

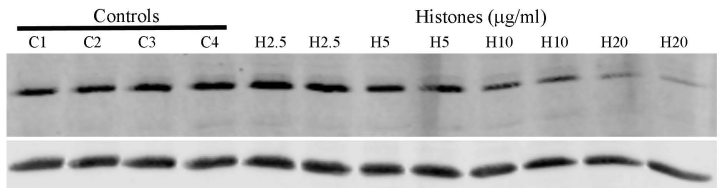

Legend 3 – Histones inhibit neurite outgrowth by an YB-1 mediated mechanism. A. Cortical neurons treated with mixed Histones, H3 or H4 (2.5,5, or 10µg/ml) induce elevation in phosphorylated YB-1 (pYB-1), normalized to YB-1 and Actin levels. **B.** Overexpressing the YB-1 plasmid in cortical neurons by NEON transfection and plating in microfluidic chambers results in shorter neurite outgrowth in a dose dependent manner as determined by β-III-tubulin staining. **C.** Cartoon of a microfluidic chamber diagrammatically showing where we apply the histones or to the neurites and then lysed the cell bodies 48 hours later, on the opposing side. Cortical neurons plated in microfluidic chambers for 4-5 days grow long neurites across the microgroove. Using histones or fluorescent microbeads that are covalently coupled to histones (or non-coupled for controls) and too large to cross the microgrooves, or with 10 or 20µg/ml mixed Histones (His10 or His20) are applied to the neurite compartment (axonal) only and we wait 48hours before lysing the cell body compartment (somal) with 2XRIPA buffer and run a western blot. We detect elevation of pYB-1 in the cell bodies normalized to GAPDH. **D1.** Non-coupled beads (green) had no effect on neurite outgrowth (β-III-tubulin in red), higher magnification in **D3. D2**. Histone-coupled beads (green) appear more aggregated compared to non-coupled beads and significantly inhibited neurite outgrowth, higher magnification of the beaded BIII-tubulin (red) with histone-coupled beads in **D4. E.** To confirm if pYB-1 are elevated after injury inducing histone release in the ONC, we crushed the axons of the optic nerve and 48hrs later collected the retinal cell layer (Ipsi 1&2) and collected the retinal layer of the non-injured side (Contra 1&2) in the same animal and prepared them for western blots. We found significantly elevated levels of pYB-1 on the injured (Ipsi) side compared to the non-injured (Contra) side. **F.** Histone applied to cortical neurons induces activation of Rho GTPase, the positive control for the kit was the GTP-γs. **G.** Histone applied to cortical neurons results in dose dependent decrease (2.5-20µg/ml) in p35 levels without any detectable p25.